MEFISTO

General objectives: combine atomistic and dislocation modelling techniques with detailed experiments of irradiation and thorough post-irradiation examination, in order to:

- Study mechanisms of formation of Cr-NiSiP clusters to predict their kinetics and stability and in general nanostructural evolution in FeCrX alloys (*where X stands for any additional alloying element or series of them*)

- Study the interaction of the generated nanostructure with dislocations and its correlation with radiation induced hardening

The reason for focusing on these objectives is that these Cr-NiSiP clusters seem to be the features mainly responsible for radiation-hardening in F/M steels and bear strong resemblance with similar clusters observed ubiquitously in current reactor pressure vessel steels, being recognised as the main cause of hardening and embrittlement.

Tasks:

2.1 Development of models describing formation of Cr-Ni-Si-P clusters in Fe-alloys
2.2 Study of effect of Cr-Ni-(Si/P) clusters on radiation hardening
2.3 Microstructural examination of irradiated Fe-Cr-(NiSiP) alloys and assessment of the corresponding irradiation hardening as validation and guide for the models

Objectives for the period:

Task 2.1
- Produce dataset of DFT calculations on solute/solute and defect/solute interaction, small precipitate stability, as well as mobility of solutes in Fe alloys
- Develop empirical interatomic potential for bcc FeCrNi
- Set the basis for the development of suitable kinetic Monte Carlo models describing formation of Cr-NiSiP clusters under irradiation

Task 2.2
- (*Will start after the interatomic potential is properly validated*)

Task 2.3
- Selection, procurement and first characterization of materials to be investigated
- Performance of neutron and ion irradiations
- Detailed plan of post-irradiation characterization of selected model alloys

Task 2.1

DFT calculations aimed at determining parameters to fit a bcc FeCrNi(Si/P) interatomic potential, as well as AKMC models, were produced by KTH and EDF-R&D. They mainly concerned solute/solute & defect/solute interactions in an Fe matrix, including interactions between multiplets of solutes. A wealth of data are now available to fit and validate an FeCrNi(Si) bcc potential (see Fig. 2.1 for examples of data), as well as DFT-based multicomponent AKMC models.

The mobility of Cr, Ni, Si, P, as well as Mn and Cu, via vacancy and/or interstitial mechanism has been studied combining DFT & AKMC or using SCMF theory by KTH and CEA, leading to a first publication

[L. Messina, P. Olsson, M. Nastar, T. Garnier, C. Domain, PRB 90, 104203 (2014)] and more are to come. Conclusions from this work:

- All solutes that form aggregates under irradiation, except Cr, are dragged by vacancies at temperatures of technological interest
- Mn, P and Cr are also transported by self-interstitials

All DFT-based results will be reported in deliverable D211.

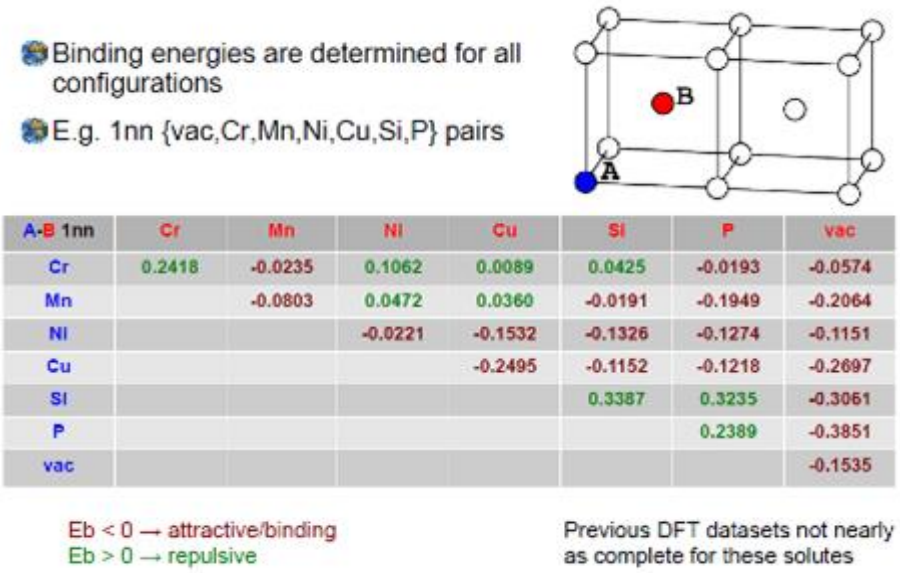

A-B 1nn	Cr	Mn	Ni	Cu	Si	P	vac
Cr	0.2418	-0.0235	0.1062	0.0089	0.0425	-0.0193	-0.0574
Mn		-0.0803	0.0472	0.0360	-0.0191	-0.1949	-0.2064
Ni			-0.0221	-0.1532	-0.1326	-0.1274	-0.1151
Cu				-0.2495	-0.1152	-0.1218	-0.2697
Si					0.3387	0.3235	-0.3061
P						0.2389	-0.3851
vac							-0.1535

Fig. 2.1a – DFT data on solute-solute and solute-vacancy pair interaction in Fe.

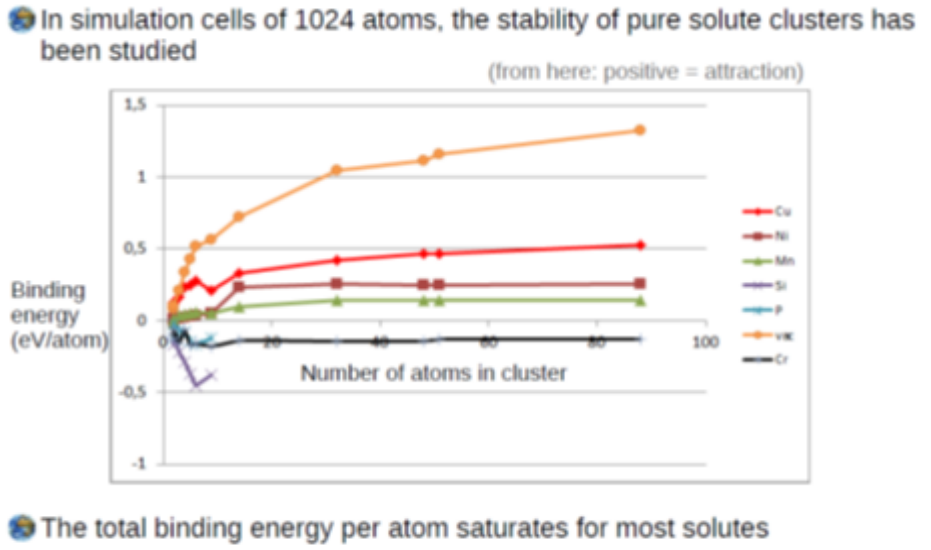

Fig. 2.1b – DFT data on solute-solute interaction in Fe for large solute clusters.

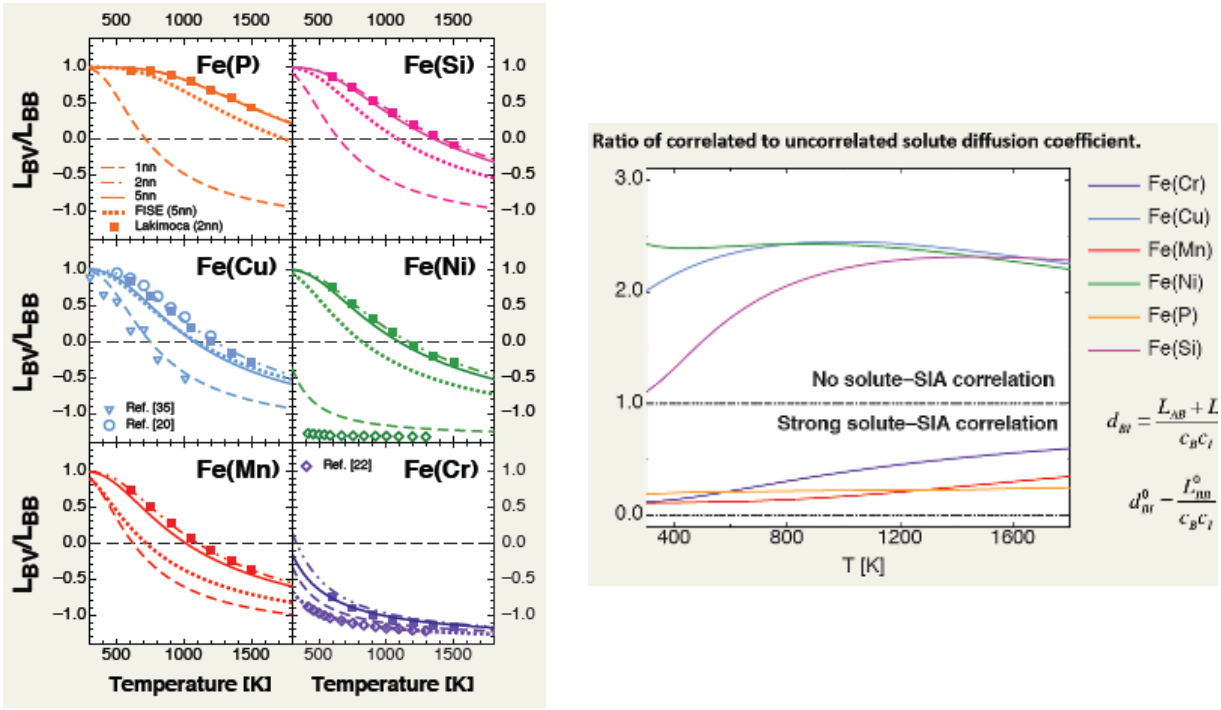

Fig. 2.2 – Vacancy dragging of solutes (left) and correlation of self-interstitial atom (SIA) with solutes in Fe according to the SCMF study.

The development of an interatomic potential for bcc FeCrNi(Si) is being pursued step-by-step by SCK•CEN:

- The FeNi potential has been refitted to remove some shortcomings of the older FeNi potential concerning interaction with vacancies; also the solubility limit is better reproduced; fcc intermetallic stability is lost but this is not really of relevance for the problem treated here;
- The FeCrNi potential (which is the deliverable for the present project) has been issued (Milestone MS211), but needs validation: this will be the task of HZDR; the validated potential will be fully reported in Deliverable D212;
- The fitting of an FeCrNiSi potential will be also attempted later: even though originally not foreseen as part of this project, if successful it will be an important step forward, allowing the study of the mechanism of formation of CrNiSi clusters.

Advanced kinetic Monte Carlo models are being developed step-by-step to describe the formation of Cr-Ni-Si-P clusters in Fe-alloys under irradiation, as well as to describe the Fe-Cr-C system, with the involvement of several groups (U. Alicante, SCK·CEN, CEA):

- At SCK•CEN an OKMC "grey alloy" model for FeCrC has been developed, as a first step and basis for the subsequent explicit introduction of solute atoms transported by point-defects, using the results of the above-mentioned DFT-based SCMF study. The model, which is physically based and largely uses as input the results of atomistic simulations performed over the last decade in the framework of several European projects, demonstrates and explains especially two effects:

  - ❑ The addition of Cr to Fe reduces the vacancy concentration as compared to pure Fe (at comparable dose), mainly because of the effect of Cr on reducing

interstitial cluster mobility, leading to enhanced recombination. Cr therefore leads to swelling suppression, in agreement with experiments (see Fig. 2.3).

- ❑ Density and size of interstitial dislocation loops visible in TEM decrease progressively with Cr addition, as observed experimentally, also as a consequence of the reduced mobility of interstitials and enhanced recombination

The model also allows the effect of C content in the matrix to be accounted for, revealing that the low value of the latter allows the Cr effect to be dominant. A paper has been submitted [M. Chiapetto, L. Malerba, C.S. Becquart, submitted to J. Nucl. Mater. (2015)].

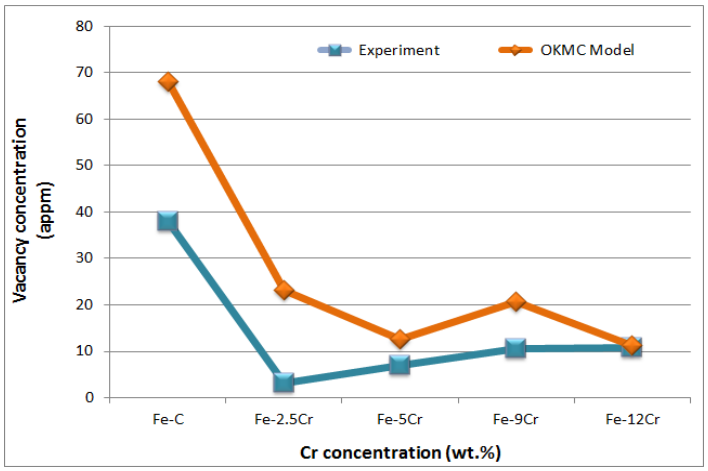

Fig. 2.3 – Reduction of vacancy concentration after neutron irradiation to ~0.06 dpa in BR2 (same flux) as a function of Cr content: the model catches acceptably well the experimental trend (from positron annihilation spectroscopy).

- The U. of Alicante is developing, with the in-kind support of IMDEA Materials, a "cellular" OKMC model. The specificity of this model is that the simulation volume is divided in cells with different nominal Cr concentrations (see Fig. 2.4). This allows parameters that depend explicitly on local Cr concentration to be used to describe point-defect cluster evolution, while also describing radiation-enhanced & radiation induced precipitation in the binary alloy. The methodology is established and the code ready, but the model needs more extensive testing.

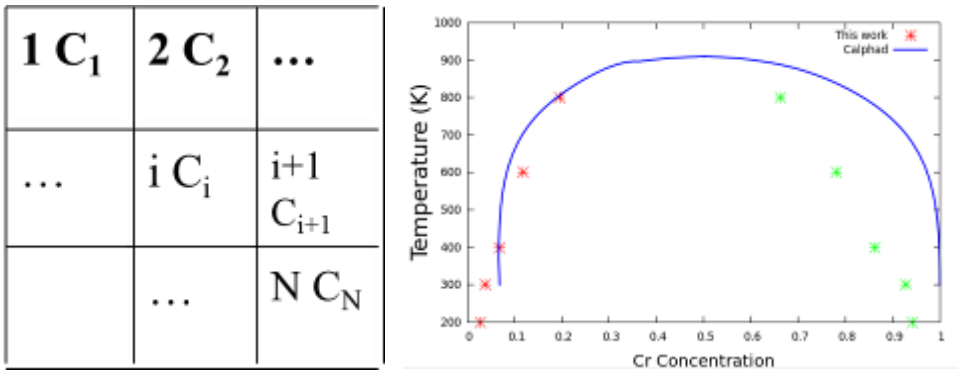

Fig. 2.4 - Left: Schematic description of the concept of "cellular" OKMC: simulation volume divided into cells with different alloy concentrations, *C*. Right: Phase diagram calculated with Cell-OKMC.

- CEA is developing an AKMC model for FeCrC focused on studying the atomistic details of segregation of Cr in Fe (with and without carbon) on grain boundary and possibly loops, model fitted to DFT data. Although looking at the same system as the above models, this one contains atoms explicitly, so it can be used as a benchmark and provider of parameters for the two above models. An interesting result of the model, in agreement with experiments, is the fact that Cr segregation at grain boundaries is the consequence of competition between vacancy-mediated (taking Cr away from sinks) and interstitial-mediated (taking Cr to sinks) solute diffusion, the latter being dominant at lower temperature, the former at higher temperature (see Fig. 2.5).

It is expected that the final model describing the formation of CrNiSiP clusters in (non-pure) FeCr alloys will contain elements of all three models currently addressed in parallel in order to separate problems and difficulties.

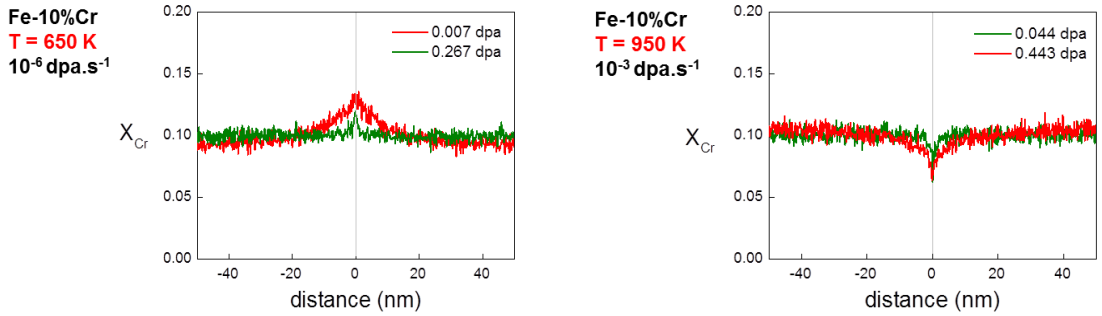

Fig. 2.5 - Left: Cr segregation at grain boundary via dominating interstitial-mediated diffusion (650 K). Right: Cr- depletion at grain boundary via dominating vacancy-mediated diffusion (950 K).

Task 2.2

(will start later in the course of the project, when the interatomic potential is validated)

Task 2.3

The materials to be used for the modelling-oriented experimental programme have been selected and produced. They are listed in Table 2.1: they are basically ferritic Fe-Cr alloys of industrially-controlled purity (produced by OCAS, Belgium) that contain also, in different proportions, small amounts of Ni, Si and P. These alloys have been dispatched to four laboratories, namely CIEMAT, HZDR, SCK•CEN and CNRS/GPM. A selection of these alloys is meant to be both neutron- and ion-irradiated, as summarised below. In addition, three F/M steels (from archive heats available at SCK•CEN) and ultra-high purity Fe-Cr-C alloys (fabricated years ago in very small quantity by the École des Mines,Saint Étienne, France, in the framework of fusion research -EFDA- available at CEA) are included in the matrix of materials for experiments in this WP (see Table 2.2 for the latter). See Milestone MS231 for more details.

A plan of neutron and ion irradiation has been elaborated for the alloys in Table 2.3.

The neutron irradiation campaign was performed in two BR2 cycles (in-kind contribution of SCK•CEN), during 2014-15 (before BR2 refurbishment) in the Callisto loop where water circulates at ~290°C, in the in-pile section IPS3, reaching a dose <0.1 dpa (dosimetry still pending). Six alloys where irradiated at the water temperature, eight alloys (including the previous six) at ~450°C, using a He gap and γ heating (see Table 2.3). An additional neutron irradiation of tensile specimens, including the steels of Table 2.1, but also other F/M steels, was performed, as well: this second irradiation took place close to a fuel element, reaching significantly higher dose (~0.7 dpa), although for a limited amount of specimens only.

The ion irradiation campaign is planned at the Ion Beam Center of HZDR (in-kind contribution) using 5 MeV Fe^{+1} ions, in three groups of alloys (see box 2.1): the first group of alloys was already irradiated, as planned; the second and third group will be irradiated soon, probably at the end of the present reporting period.

In addition, selected Fe-Cr (C) alloys were irradiated under similar conditions with electrons (CEA, in-kind contribution): Fe-15at%Cr alloy during 2h, 3h or 5h at 250°C, 300°C and 400°C.

All details about the irradiation campaigns will be given in Milestone MS233, after the second group of alloys is ion irradiated.

Alloy	Grain size (µm)	σ_y (MPa)	σ_u (MPa)	ε_u (%)	ε_f (%)	HV10
Fe	95	196	303	17	33	58
Fe5Cr	36	205	310	19	39	77
Fe5Cr0.1Ni	37	180	300	24	46	82
Fe5Cr0.2Si	37	197	323	24	45	83
Fe5Cr0.03P	36	221	325	19	37	88
Fe5CrNiSiP	31	231	353	21	40	102
Fe9Cr	25	252	391	17	35	110
Fe9Cr0.1Ni	24	246	379	19	40	104
Fe9Cr0.2Si	27	242	378	20	39	103
Fe9Cr0.03P	26	237	373	20	39	101
Fe9CrNiSiP	27	257	399	20	38	113
Fe14Cr	241	230	306	17	31	105
Fe14Cr0.1Ni	240	250	319	18	32	113
Fe14Cr0.2Si	217	248	319	18	31	112
Fe14Cr0.03P	253	263	343	17	30	114
Fe14CrNiSiP	239	268	319	10	20	123
T91	14	577	716	7.7	25	229
P92	31	498	672	10.4	26	213
E97	6	547	681	6.3	25	220

Table 2.1 – List of ferritic alloys with nominal composition and basic mechanical and microstructural features: grain size, yield strength, ultimate tensile strength, uniform and total elongation, and Vickers hardness. Three F/M steels are also included in the list.

Short name	Cr w.%
Fe-10Cr	10.1
Fe-10CrC	10.1
Fe14Cr	14.25
Fe-18Cr	17.97

Table 2.2 – List of ultra-high pure Fe-Cr-C alloys included in the experimental programme.

A detailed workplan of characterization involving CIEMAT, CNRS, HZDR, SCK•CEN and CEA, as well as ENEA (limited to previously neutron-irradiated F/M steels) has been made and is provided in Milestone MS232.

For what concerns neutron-irradiated materials, the summary of the planned microstructural characterization is indicated in Table 2.3. In addition, tensile tests, hardness and internal friction, in-

situ TEM straining, nanohardness and gamma-induced PAS are foreseen. However, none of these will start until the specimens are definitively out of the reactor and dispatched.

For what concerns ion- (and electron) irradiated materials, the characterization will involve CEA, CIEMAT, CNRS and HZDR and encompass APT, PAS, TEM and nanoindentation.

290°C		~450°C	
		Fe	PAS, TEM
Fe-5Cr-NiSiP	SANS	Fe-5Cr-NiSiP	PAS, TEM, SANS
Fe-9Cr		Fe-9Cr	PAS, TEM
Fe-9Cr-NiSiP	SANS	Fe-9Cr-NiSiP	PAS, TEM, APT, SANS
Fe-14Cr-NiSiP	APT, SANS	Fe-14Cr-NiSiP	PAS, TEM, APT, SANS
Fe-9Cr (Mart.)		Fe-9Cr (Mart.)	PAS, TEM
Eurofer97		Eurofer97	PAS, TEM, APT
Optifer*	SANS	T91	PAS, TEM, APT
ORNL(9Cr2WVTa)*	SANS		

Table 2.3 – List of materials irradiated in BR2 at two different temperatures, dose <0.1 dpa, and relevant microstructural characterisation according to plans. *Optifer and ORNL(9Cr2WVTa) steels come from previous irradiation campaigns but will be characterised as part of the WP2 of MatISSE.

Group 1: Fe9CrNiSiP, Fe9Cr, Fe9Cr (GETMAT), Fe5CrNiSiP, Fe14CrNiSiP, Fe
0.5 dpa @ T = 200°C, 300°C and 450°C
+ In-situ straining at 300°C

Group 2: Fe9Cr, Fe9CrNi; Fe9CrP, Fe9CrSi; Fe9CrNiSiP, Fe
Groupe 3: Fe14Cr, Fe14CrNi; Fe14CrP, Fe14CrSi; Fe14CrNiSiP
0.1 dpa @ T = 300°C

Box 2.1 – Groups of alloys to be ion-irradiated and relevant conditions.

MOIRA

Task 2.4

The analysis of mechanisms of irradiation creep according to what is known from the literature for a range of steels (not only F/M but also austenitic and ODS) culminated in a substantial report, made of a main part and two appendices, with the contribution of KIT, PSI and CEA. This report is available as Deliverable D241.

Task 2.5

This tasks aims essentially at obtaining detailed information from atomistic simulation techniques about how the application of stress influences the properties of radiation defects in bcc Fe.

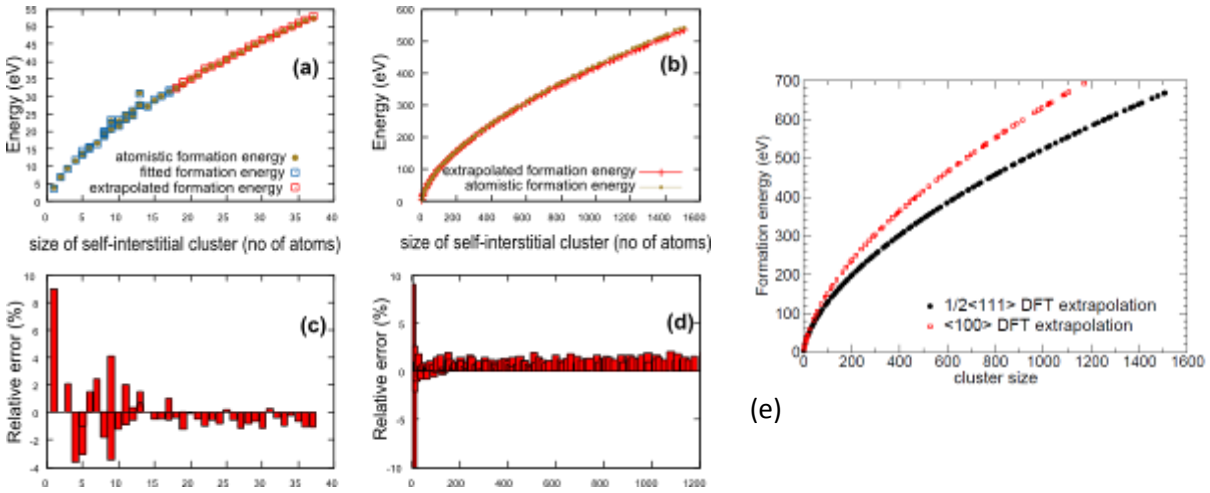

Fig. 2.7 – Analytical model describing formation energy of self-interstitial clusters in Fe. (a-d): validation by comparison with results of atomistic simulations using an empirical potential. (e): parameterization on ab initio data.

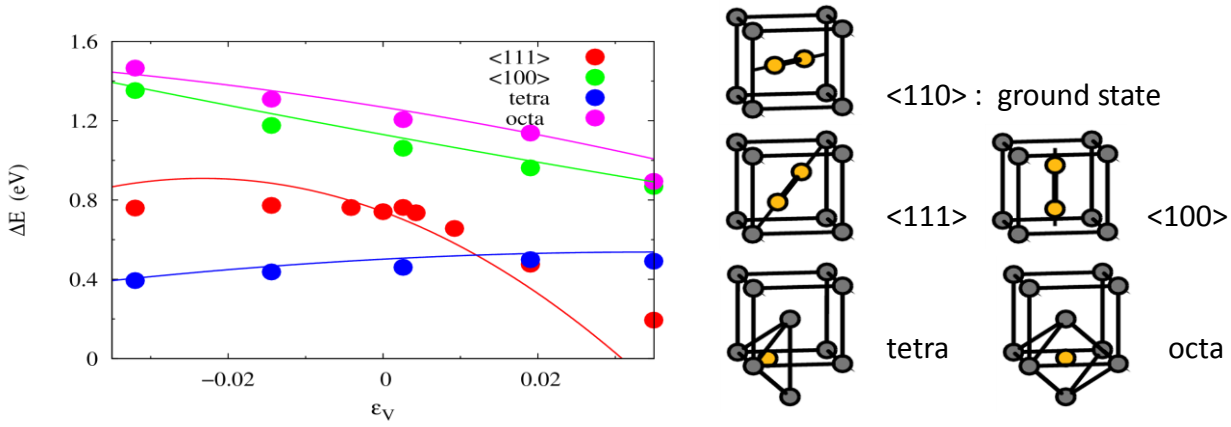

Fig. 2.8 – Variations with an applied hydrostatic strain of the of the formation energy of a self-interstitial in iron for its various configurations. Symbols are results of ab initio calculations and continuous lines correspond to predictions of the elastic modelling.

CEA developed a new expression to calculate the formation energy of interstitial dislocations loops, validated with empirical potentials and then parameterized on DFT data (Fig. 2.7). A model to include the effect of the variation of the formation energy with applied stress is under development. In parallel, formation and migration energies of point defects under applied stress have been calculated by DFT and the data used to validate and parameterize elastic models (Fig. 2.8), that can be used at upper scales: this should also eventually allow diffusion coefficients under applied stress to be obtained by KMC techniques.

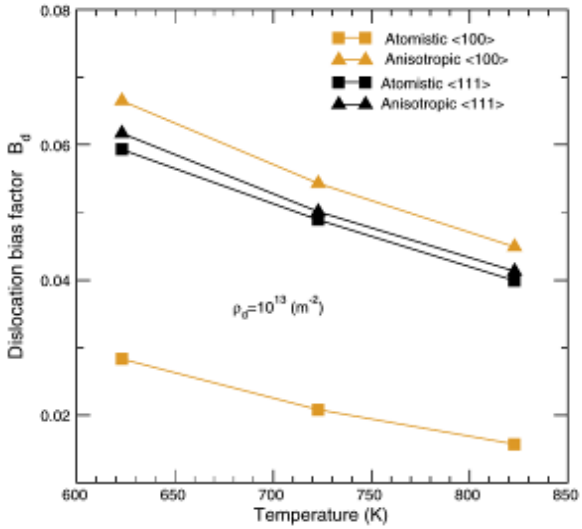

Fig. 2.9 – The dislocation bias of both types edge dislocations in bcc iron. <100> and <111> represent <100>{001} type and ½<111>{110} type, respectively. Results of atomistic simulations are compared to prediction of anisotropic elasticity (from Z. Chang, D. Terentyev, N. Sandberg, K. Samuelsson, P. Olsson, J. Nucl. Mater. 461 (2015) 221-229)

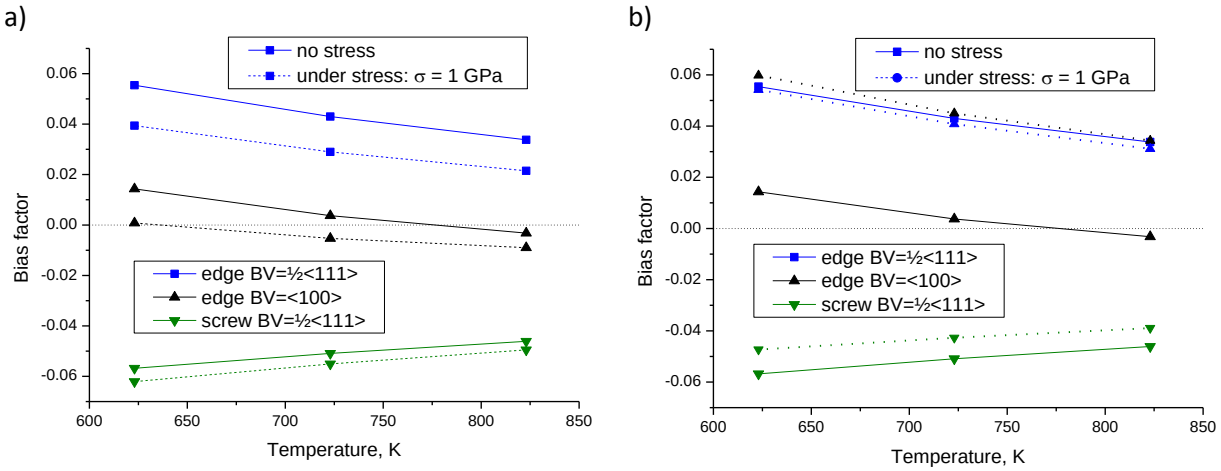

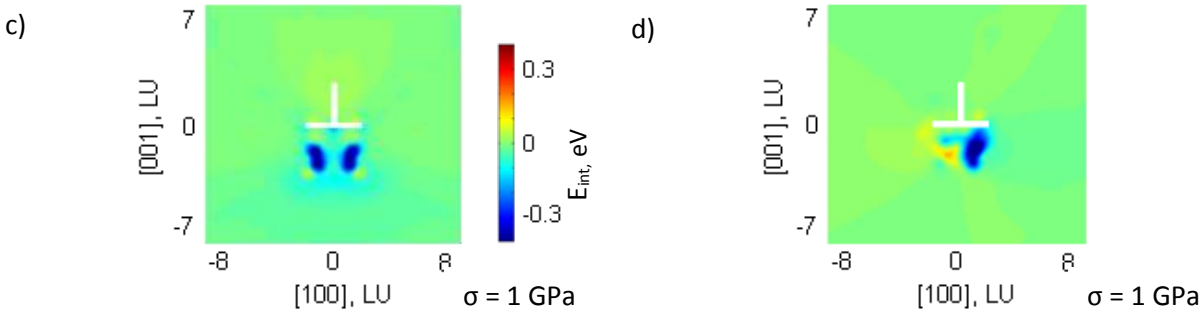

Fig. 2.10 – Variation of the dislocation bias factor with applied expansive (a) and compressive (b) hydrostatic stress for dislocations of different type and Burgers vector (BV). Difference between the interaction energy of a self -interstitial atom with a <100>{001} edge dislocation under isotropic expansion (c) and shear stress (d) to the corresponding interaction energy without external stress. Negative and positive values describe attraction and repulsion , respectively

The dislocation bias is the parameter that expresses the more favourable absorption of interstitials versus vacancies by dislocations. A method that uses a combination of atomistic techniques, elasticity theory and finite element calculations to calculate this bias has been developed by KTH and SCK•CEN. Initially applied to fcc metals such as Cu, Ni, Al, calculations have been now done also for bcc Fe, leading to a publication [Z. Chang, D. Terentyev, N. Sandberg, K. Samuelsson, P. Olsson, J. Nucl. Mater. 461 (2015) 221-229] (Fig. 2.9). This method has been taken over by HZDR, with the support of SCK•CEN and KTH, to analyze the effect of the external stress (isotropic compression or expansion and shear stress) on the dislocation bias factor in bcc Fe. The influence of the applied load on the bias factor has been thoroughly quantified and rationalized on the basis of the observed modification of the dislocation-defect interaction energy landscape (Fig. 2.10).

Other activities, not started yet but that will be considered, along the same line of addressing stress effects on defect properties, are: (i) study of the mobility of glissile loops in presence of stress; (ii) study of slip bands in interaction with nanostructural defects.

Task 2.6

CEA is working on the derivation of irradiation creep constitutive laws at the crystal and polycrystal scales based on physical mechanisms, for implementation in FE codes. A set of continuum evolution equations obeyed by free dislocation densities has been written. These equations are coupled with point defects evolution through climb equations and will be introduced in a cluster dynamics code. The model, first developed for fcc austenitic stainless steels (Fig. 2.11), need to be adapted now to bcc steels and to describe the variation of the time evolution of the dislocation density under irradiation.

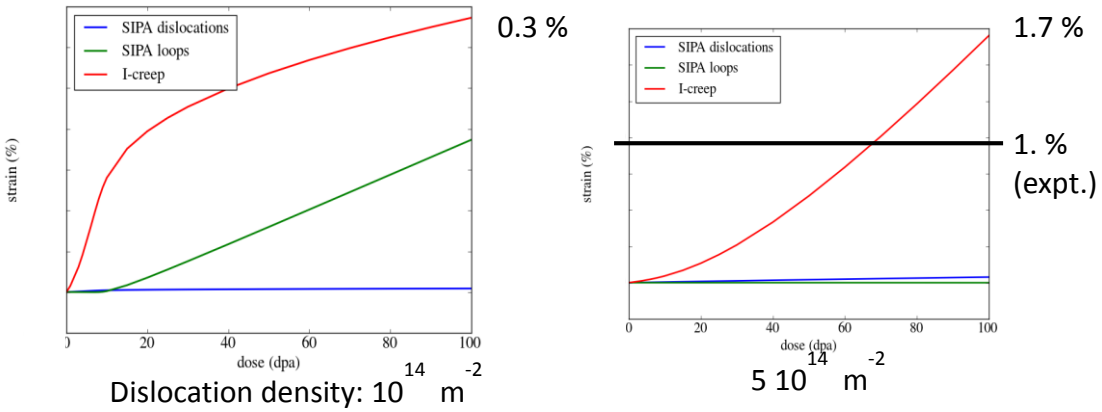

Fig. 2.11 – Variation of the plastic strain with the irradiation dose in an austenitic stainless steel for two different fixed dislocation densities, considering various irradiation creep mechanisms.

Publications and presentations (non-exhaustive list):

NO.	Title	Main author	Title of the periodical or the series	Number, date or frequency	Year	Pages	Permanent identifiers[1] (if available)
1	*Surface damage in TEM thick alpha-Fe smaples by implantation with 150 keV Fe ions*	*M. J. Aliaga*	*Nuclear Instruments and Methods B*	*Vol. 352*	*2015*	*217-220*	doi:10.1016/j.nimb.2014.11.111
2	*Exact ab initio transport coefficients in bcc Fe−X (X=Cr, Cu, Mn, Ni, P, Si) dilute alloys*	*L. Messina*	*Phys. Rev. B*	*Vol. 90*	*2014*	104203	doi:10.1103/PhysRevB.90.104203
3	*Anomalous bias factor of dislocations in bcc iron*	*Z. Chang*	*J. Nucl. Mater.*	*Vol. 461*	*2015*	221-229	doi:10.1016/j.jnucmat.2015.03.025
4	*Modeling radiation induced segregation in Fe-Cr alloys*	*O. Senninger*	*Acta Mater*		*submitted*		
5	*Effect of Cr content on the nanostructural evolution of irradiated ferritic/martensitic alloys: an object kinetic Monte Carlo model*	M. Chiapetto	J. Nucl. Mater.		*submitted*		

[1] A permanent identifier should be a persistent link to the published version full text if open access or abstract if article is pay per view) or to the final manuscript accepted for publication (link to article in repository).

Conference Name	Date	Location	Authors	Title	Type of presentation (oral/poster)
MRS Spring Meeting Symposium XX: Multiscale Modeling and Experiments on Microstructural Evolution in Nuclear Materials	April 6 – 10 2015	San Francisco	F. Soisson	Kinetics of Precipitation in Fe-Cr and Fe-Cr-C Alloys under Irradiation	oral
MRS Fall meeting 2014 Symposium DD: Materials for Advanced Nuclear Technologies	November 30 December 5, 2014	Boston	F. Soisson	Kinetics of segregation and precipitation in Fe-Cr alloys under irradiation	oral
Multiscale Materials Modeling 2014	October 6-10, 2014	Berkeley, USA	M. J. Aliaga, M. J. Caturla, I. Martín-Bragado, L. Malerba	Combined molecular dynamics and object kinetic Monte Carlo simulations of ion implantation in Fe thin films	oral
Multiscale Materials Modeling 2014	October 6-10, 2014	Berkeley, USA	D. Murali, M. Posselt, M. Schiwarth	First-principles study of the free energy of point defects and their clusters in bcc-Fe	oral